Available online at www.sciencedirect.com
ScienceDirect
Journal of Molecular Catalysis A: Chemical 281 (2008) 126–136
JOURNAL OF MOLECULAR CATALYSIS A: CHEMICAL
www.elsevier.com/locate/molcata

Development and vapor sorption assessment of dimorphic SiO_2 porous substrates

C. Velásquez [a], M.L. Ojeda [b], A. Campero [a], J.M. Esparza [a], F. Rojas [a,*]

[a] *Departamento de Química, Universidad Autónoma Metropolitana-Iztapalapa, P.O. Box 55-534, México D.F. 09340, Mexico*
[b] *Instituto de Química, Universidad Nacional Autonoma de México, Circuito Exterior, Ciudad Universitaria, México DF 04510, Mexico*

Available online 28 July 2007

Abstract

Dimorphic SiO_2 pore substrates (i.e. mesoporous solids made of separated grains of cylindrical and spherical void entities) are synthesized from several possible silicon alkoxide sol–gel routes in the presence of triblock copolymer surfactants that act as pore templates. The preparation method consists in bringing together colloidal systems in which pore-templating (spherical and cylindrical) supramolecular arrangements are dispersed within a gellifying silica matrix arising from the reaction between tetraethoxysilane and micellar aqueous dispersions of triblock copolymer surfactants. The goal is to end with a colloidal gel structure in which two kinds of micellar pore templates are repartitioned throughout the silica gel matrix. Thermal treatment of this gellifying arrangement brings about a granular porous solid of a dimorphic nature. Nevertheless, monomorphic pore arrangements can still be obtained depending on the types of surfactants and preparation conditions. Characterization of these SiO_2 adsorbents in terms of their pore structure properties is carried out by N_2 sorption, electron microscopy and X-ray diffraction.

Keywords: Dimorphic SiO_2 substrates; Two pore-shaped N_2 sorption isotherms; P123 triblock copolymer; F127 triblock copolymer; CTAB; SBA-15; SBA-16

1. Introduction

1.1. Structural aspects of dimorphous adsorbents as determined from N_2 vapor sorption

The pore size distribution, concurrently with the specific surface area, of a catalyst (or support) is of prime importance in assessing its kinetics behavior. At this respect, adsorbents endowed with a bimodal pore size distribution [1–4] are highly appreciated structures in catalysis and separation processes. This happens since this sort of substrates usually consists of micropores and mesopores (i.e. void types that can provide size, shape or adsorption selectivity toward guest molecules), which are made accessible by nearby macropore entities (i.e. voids that facilitate the transport of reactants, products or chemical species participating in the incumbent process). For instance, bimodal Al_2O_3 adsorbents have been employed for an efficient removal of dye molecules from solution [1]; in contrast, unimodal Al_2O_3 adsorbents provide decreased adsorption separation efficiencies for the same dye extraction.

Under a rather analogous context, adsorbents of a *dimorphic* nature (i.e. porous solids endowed with two types of void shapes distributed throughout the grains comprising a granular solid) would surely represent interesting perspectives for a number of physicochemical processes. The following substrates can be considered as precursors of this kind of dimorphic porous adsorbents: (i) the pitch-based carbons [3] imprinted by spherical voids as well as by the hollow spaces existing between contiguous cylindrical rods in hexagonal arrangement, (ii) the carbon adsorbents arising from a templating procedure that involves ordered SBA-15 and disordered (globular) silica pore templates [2].

1.2. Pore structure modeling and possible sorption behavior of dimorphous substrates

From a pore modeling point of view, dimorphous adsorbents can be considered as a collection of pore assemblies (granules or domains), each one of these made by a given type of pore shape, that are mixed throughout the adsorbent with another pore shape. Under the appropriate pore shape and size circumstances, dimorphous substrates constitute ideal substrates for testing the theorems advanced by the *independent pore domain theory of sorption hysteresis* (IPDTSH) [5]. If a porous solid is comprised

* Corresponding author. Tel.: +52 55 58044672; fax: +52 55 58044666.
E-mail address: fernando@xanum.uam.mx (F. Rojas).

1381-1169/$ – see front matter © 2007 Elsevier B.V. All rights reserved.
doi:10.1016/j.molcata.2007.07.040

by separate regions of two sorts of voids displaying dissimilar but simple shapes (e.g. cylindrical and spherical), the resultant sorption isotherm likely portrays a great deal of useful characteristics that could eventually allow a plain identification of the geometrical pore shapes that compose the solid. At this respect, the *adsorption* (AB) and *desorption* (DB) *boundary curves* that delimit the *hysteresis loop* (HL) of the sorption isotherm can each undergo different slope evolution through their extents, as will be shown in this work.

From a performance point of view, each pore shape existing in dimorphous substrates assumes an independent but a concomitant role during the development of the sorption and capillary processes that can take place in this kind of structures. On the one hand, monolayer–multilayer adsorption of vapor molecules occurs simultaneously on the surface of both types of pore shapes at low pressures. On the other hand, capillary condensation arises (in general) at different vapor pressure intervals in each type of pore shape, in view of the different geometrical shapes (i.e. curvatures) of the voids and therefore of the liquid–gas interfaces that are developed during the uptake of the adsorptive molecules. Assuming that capillary condensation is taking place in a porous solid made of spherical and cylindrical capillaries of the same diameters, and accepting that the classical Kelvin equation is appropriate to describe this process (thus neglecting the influences of the thickness of the adsorbed layer and of the adsorption potential), condensation in spherical pores occurs at a relative vapor pressure, $(p/p^0)_{sph}$, lower than that associated to the filling of the cylindrical voids $(p/p^0)_{cyl}$ (i.e. $\left(p/p^0\right)_{sph} = \left(p/p^0\right)^2_{cyl}$. Additionally, the tubular pores can be emptied of condensate irrespective of what happens in the spherical entities, ever since the former voids are not being blocked in their direct access to the vapor phase while the latter pores are interconnected to each other by small necks, something that seriously obstructs the evaporation of their condensate phases. Another factor that can be inherent to dimorphous adsorbents is the different adsorption potential existing inside each pore type: if, at a given p/p^0, vapor molecules are adsorbed on the interior surface of a spherical cavity, the adsorption potential emanating from the solid walls toward the ad-molecules is higher than that emitted by the surface of a cylindrical void of the same diameter [6]. These unequal adsorption potentials existing in the pores of dimorphous structures could be a key factor for successfully achieving the separation of flowing gas mixtures formed by substances of related physicochemical characteristics, e.g. ethane–ethylene, propane–propylene, etc.

When having a double distribution of pore shapes within a dimorphous solid, the experimental determination of the so-called sorption scanning curves [5] can shed some light upon the intensities of the two types of sorption hysteresis that have so far been recognized: pore hysteresis and pore network hysteresis.

The present work is organized as follows. Experimental details concerning the preparation of dimorphic SiO_2 porous substrates are firstly provided; these include information about individual preparations of the SBA-15 and SBA-16 silica substrates, which are mixed together in order to create a reference dimorphic pore material. Afterward, N_2 sorption isotherms at 76 K (i.e. boiling point of N_2 at Mexico City) on dimorphic SiO_2 adsorbents are shown and the particularities of these curves are made evident. Finally, pore size distribution analyses of SiO_2 dimorphic structures are undertaken and relevant conclusions about the nature and properties of dimorphous SiO_2 substrates are summarized.

2. Experimental

2.1. Materials

The preparation of SBA-15, SBA-16, and dimorphic SiO_2 adsorbents require of the following chemical reactants that can be used as supplied without further purification: tetraethylorthosilicate (TEOS, Aldrich 98%), ethanol (Aldrich, 99.8 wt.%), Pluronic F127 and Pluronic P123 triblock copolymers (BASF Corp.), and HCl (37 wt.% in H_2O, Sigma–Aldrich). Pluronic F127 is an ABA triblock copolymer of the general formula $(EO)_{106}(PO)_{70}(EO)_{106}$ that is composed by polyethylene oxide (EO) and polypropylene oxide (PO) chains. In turn, P123 is an ABA triblock copolymer of general formula $(EO)_{20}(PO)_{70}(EO)_{20}$. A third surfactant, cetyltrimethylammonium bromide (CTAB), was bought from Aldrich and crystallized (~99% purity). N_2 and He gases of ultra-high-purity (99.999%; Praxair) were employed to measure the N_2 sorption isotherms on all dimorphous and reference silica materials.

2.2. Preparation of SBA-16 silica [6]

Pluronic F127 [1.6 g (1.26×10^{-4} moles)] was mixed with 2.6 cm^3 of HCl 0.037 M. Afterward, a volume of 12.2 cm^3 (0.2096 moles) of ethanol was incorporated under stirring to the above surfactant mixture in order to attain a homogeneous solution. Subsequently, an amount of 3.6 cm^3 of TEOS was added drop-by-drop to the surfactant solution while keeping the system under stirring for further 5 h. The theoretical molar composition of the ensuing sol was: 1 TEOS: 9 H_2O: 0.006 HCl: 13 EtOH: 0.008 F127. Finally, the above sol was left to gellify at room conditions during 2 weeks. Eventually, a monolithic (transparent) specimen was obtained; the solid was washed with distilled water and cut into several pieces and finally treated at 500 °C during 6 h in an oven (a heating ramp of 1 °C min^{-1} was followed).

X-ray diffraction (XRD) patterns of the SBA-16 sample were obtained via a Siemens D500 instrument. N_2 sorption isotherms (boundary and scanning curves) at 76 K were measured with a Quantachrome Autosorb-1 LC instrument. The solid was outgassed overnight at 200 °C. TEM images of the SBA-16 material were taken by means of a JEM-2010F FASTEM instrument.

2.3. Preparation of SBA-15 silica [6]

The SBA-15 SiO_2 material was synthesized as follows. A mass of 1.5 g of Pluronic P123 block copolymer was dissolved in 48 cm^3 of a solution of HCl 2M. The temperature was then raised to 50 °C and a volume of 3.7 cm^3 of TEOS was added drop-by-drop to the above mixture while subjecting the sys-

tem to a vigorous stirring during 5 min. The stirring rate was then lowered down and kept under this condition for further 24 h. Subsequently, the reaction beaker holding the gelling mixture was placed on top of a sand-containing heating mantle and taken to 80 °C for approximately 48 h. The ensuing white precipitate was separated from the liquid phase by filtering and washed abundantly with deionized water. Afterward, more residual surfactant was removed from the as-synthesized solid product by slurring it in 40 cm^3 of a 50 vol.% ethanol/H_2O solution for 2 h, after which time it was once more filtered and washed with distilled water, dried at 100 °C and finally calcined in air for 6 h at 550 °C (heating rate 1 °C min^{-1}). The nominal molar composition of the as-synthesized gel was 1 TEOS: 158 H_2O: 6 HCl: 0.016 Pl23. The resultant SBA-15 material was characterized by TEM employing a Zeiss EM-910 electron microscope operated at 120 kV. N_2 sorption isotherms (boundary and scanning curves) at 76 K were measured by means of a Quantachrome 1L-C automatic volumetric instrument. The SBA-15 sample was degassed at 250 °C for 8 h prior to the adsorption run.

2.4. Preparation of a reference dimorphic material from the mechanical mixing of SBA-16 and SBA-15 SiO_2 substrates

In order to observe the N_2 sorption characteristics of a dimorphic SiO_2 adsorbent, a mixture of SBA-16 and SBA-15 phases was prepared as follows: 0.024 g of the SBA-16 silica was mixed with 0.09 g of the SBA-15 substrate. The preceding mesoporous hybrid silica material was characterized by N_2 sorption and X-ray diffraction (XRD).

2.5. Preparation routes of dimorphous SiO_2 substrates

The preparation of dimorphous pore substrates (i.e. mesoporous solids made of a mixture of separate grains of cylindrical and spherical void entities) has been attempted from several possible silicon alkoxide sol–gel routes in the presence of two triblock copolymer surfactants acting as pore templates. Essentially, the preparation method consists in bringing together either aged or incipiently aged colloidal systems in which pore-templating micelles (spherical and cylindrical) are disseminated within a gellifying silica matrix arising from the reaction between TEOS and micellar aqueous dispersions of the corresponding triblock copolymer surfactants. The goal is to end with a colloidal gel structure conformed by two kinds of pore templates (i.e. cylindrical and spherical) repartitioned throughout the silica gel matrix. Thermal treatment of this gellified colloidal arrangement would bring about a porous solid of a dimorphous nature (i.e. a structure consisting of two types of void geometries, which form separate phases of each pore shape throughout the solid matrix).

Among a myriad of possibilities, four preparation routes have been devised for specifically trying to attain mesoporous substrates that are a mixture of grains, each formed by either cylindrical or spherical pore entities within a SiO_2 matrix. Each of these routes is detailed in the paragraphs below.

Route 1. Dimorphous adsorbents prepared from sol–gel systems of TEOS and aqueous mixtures of incipiently aged F127 and P123 micellar dispersions.

Initially, two colloidal dispersions (A and B) were prepared as follows:

- Dispersion A was made by placing 1.6 g of Pluronic F127 surfactant inside a glass flask and dissolved in a liquid mixture composed by 12.2 cm^3 of anhydrous ethanol and 2.6 cm^3 of 0.037 M HCl. Subsequently, a volume of 3.6 cm^3 of TEOS was added drop-by-drop to the glass flask and the ensuing sol dispersion was left aging during 4 h.
- Dispersion B was obtained by placing 1.55 g of Pluronic P123 inside a glass beaker containing 45.5 cm^3 of 2M HCl; this was followed by the dropwise addition of 3.6 cm^3 of TEOS (under these concentrations the dispersion pH value became about zero) and the resultant sol was left aging for 4 h.

Subsequently, the incipiently aged A and B dispersions were mixed together in a round bottomed flask, which was next placed on top of a sand-containing heating mantle and kept at 50 °C during 12 h. Afterward, the temperature was gradually raised to 90 °C and the surfactant-TEOS mixture was left at this condition for further 12 h. Once this time elapsed, a two-phase solid–liquid system could be observed inside the glass flask. The liquid was removed by filtration and the remnant gel was abundantly washed with distilled water and dried, firstly at room temperature for 24 h and then inside an oven kept at 70 °C for 24 h. Finally, the SiO_2 xerogel was calcined at 500 °C (heating rate of ∼0.5 °C min^{-1}) during 17 h.

Route 2. Dimorphous pore adsorbents prepared from sol–gel systems derived of TEOS and aqueous mixtures of aged P123 and incipiently aged F127 micellar dispersions.

Before proceeding to explain the particularities of this route, it is convenient to mention that the gelling kinetics of TEOS in contact with an aqueous dispersion of Pluronic F127 [7] is significantly slower than that corresponding to the system TEOS + Pluronic P123. Since the objective of this work is to attain porous substrates made of a series of separated grains of cylindrical and spherical voids, a possible good way to ensure this goal is to mix an aged TEOS + P123 micellar dispersion with an incipiently aged TEOS + F127 dispersion. The reasoning for doing is that the aged P123 silica gel mass will already include preformed cylindrical templates that will be found dispersed within the gellifying mass of the TEOS + F127 sol dispersion. In other words, the latter system will be gelling around a preformed P123-templated silica gel structure. Once again, the preparation method involved the use of two colloidal silica dispersions:

- Dispersion A was prepared by dissolving 1.55 g of Pluronic P123 surfactant in 45.5 cm^3 of 2 M HCl inside a glass beaker, the contents of which were subjected to continuous stirring. This was followed by the drop-by-drop addition of 3.6 cm^3 of TEOS (pH ∼ 0) and the sol–gel system was left aging during 4 h. The sol was then warmed to 50 °C and maintained at this temperature for 48 h for further aging.

- Dispersion B was made by placing 1.6 g of the F127 surfactant into a glass flask together with 12.2 cm^3 of anhydrous ethanol and 2.6 cm^3 of 0.037M HCl. This dispersion was vigorously stirred and kept under this circumstance during the dropwise addition of 3.6 cm^3 of TEOS. The resultant gelling system was left aging for 4 h.

Dispersions A and B were mixed together and the glass flask containing them was placed on top of a sand-containing heating mantle and the temperature was gradually increased to 90 °C. The mixture was left reacting for 48 h, after which time the contents were filtered to separate the gel phase from the liquid (sol) one. After washing repeatedly with plenty of distilled water, a hydrogel structure was finally obtained. This SiO_2 hydrogel was dried at room temperature for 24 h followed by thermal treatment at 70 °C during 24 h, and finally calcined at 500 °C for 17 h.

Route 3. Dimorphous pore adsorbents prepared from sol–gel systems obtained from TEOS and aqueous mixtures of aged F127 and P123 micellar dispersions.

The reasoning in this case was that the aged P123 and F127 gelling masses already contained preformed cylindrical and spherical templates that could be inserted within the whole SiO_2 gellified mass. The preparation method involved the use of two aged colloidal silica dispersions:

- Dispersion A was made by adding 1.6 g of the F127 surfactant into a glass beaker together with 12.2 cm^3 of anhydrous ethanol and 2.6 cm^3 of 0.037M HCl. This dispersion was vigorously stirred and kept under this circumstance during the dropwise addition of 3.6 cm^3 of TEOS. The resultant gel was left aging for 312 h (13 days).
- Dispersion B was prepared by dissolving 1.55 g of Pluronic P123 surfactant in 45.5 cm^3 of 2 M HCl inside a glass flask, the contents of which were kept under continuous stirring. This was followed by the drop-by-drop addition of 3.6 cm^3 of TEOS, a final pH ∼ 0 was attained and the sol–gel system was left aging during 4 h. The dispersion was then taken to 50 °C and maintained there for 48 h.

The F127 gel was now mixed with the P123 sol dispersion; the resultant system was taken to 90 °C and kept at this temperature for 48 h. Finally, the mixture was filtered and washed with distilled water, dried at room temperature for 24 h, dried again in an oven at 70 °C for 24 h, and finally calcined at 500 °C during 17 h.

Route 4. Preparation of dimorphous pore adsorbents from micellar mixtures of three surfactants.

This time the preparation of SiO_2 dimorphous adsorbents was attempted by including, besides the F127 and P123 triblock copolymers, a third pore template in the form of CTAB micelles. The purpose in mind was to see the possible interactions between the two surfactants (P123 and CTAB) known to render cylindrical pore templates of contrasting sizes (i.e. P123 is recognized to render larger pore diameters than CTAB) and the F127 surfactant, which was expected to provide spherical pore templates. Initially, a colloidal dispersion was prepared in the following way: a mass of 1.55 g of the P123 surfactant was mixed with 45.5 cm^3 of 2 M HCl inside a glass beaker and kept under continuous stirring until a homogeneous dispersion was formed. The previous system was left aging for 4 h, under stirring. Subsequently, 1.6 g of Pluronic F127 and 0.48 g of CTAB were added together to the preceding mixture, and finally a volume of 3.6 cm^3 of TEOS was poured to the overall system. The glass beaker and its contents were next placed on top of a sand-containing heating mantle that was kept at 50 °C for 48 h. After this time, the temperature was raised to 90 °C and maintained at this value for the next 48 h.

The resultant gel was washed repeatedly with deionized H_2O and dried at 70 °C in an oven during 24 h; finally the SiO_2 xerogel was calcined at 500 °C for 17 h (heating ramp ∼0.5 °C min^{-1}).

3. Characterization of dimorphous SiO_2 solids

3.1. N_2 adsorption

The N_2 sorption isotherms were measured in an automatic Quantachrome 1LC volumetric instrument, with N_2 as the adsorptive and He as the volume calibrating gas; both gases were purchased 99.999% UHP grade. Each SiO_2 sample was outgassed overnight at 100 °C under a vacuum of about 10^{-6} mbar.

3.2. Electron microscopy

Standard (TEM) and high-resolution (HRTEM) transmission electron microscopy studies were carried out in a Zeiss EM-910 and a JEM-2010F FASTEM electron microscopes operating at 120 and 200 kV, respectively. The samples chosen for TEM inspection were first suspended in 2-propanol and a drop of this mixture was deposited on a 300 mesh carbon-coated copper grid and subsequently dried in air before being observed.

3.3. XRD

A Siemens D-500 diffractometer coupled to a molybdenum anode X-ray tube was used to obtain the X-ray of diffraction patterns from $2\theta = 0.8°$ to 10°.

4. Results and discussion

4.1. Dimorphous SBA-15 + SBA-16 reference material

This particular reference material allows a visualization of the appearance of a sorption isotherm (see Fig. 1) that results from the combination between the uptake properties of independent spherical and cylindrical pore domains. In principle, the DB curve that is delimiting the HL of such hybrid isotherm should allow to calculate the pore size distribution (PSD) of the cylindrical mesopores given that, while these last voids are being emptied of liquid, the spherical domains remain full of condensate until cavitation [8] takes place inside them (this phenomenon usually occurs at relative vapor pressures $p/p^0 \in [0.42, 0.45]$. In turn, the AB curve that is also delimiting the HL should provide evidence about the sizes of both spherical and cylindri-

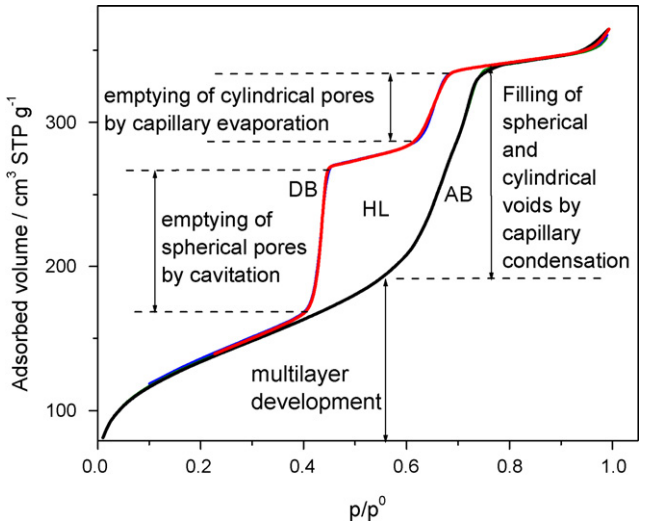

Fig. 1. Graphical aspect of the N_2 sorption hysteresis loop (HL) of a dimorphic material made of spherical and cylindrical independent pore domains. AB represents the HL adsorption boundary isotherm and DB the HL desorption boundary isotherm. Diverse sorption processes have been labeled therein.

cal pore domains, something that can sometimes be difficult to ascertain due to the possible concurrent filling of these two pore shapes.

The sorption isotherms of the SBA-15 and SBA-16 pure materials, as well as TEM photographs of the precursory SBA-15 and SBA-16 materials that make the dimorphous SiO_2 reference material, are shown in Fig. 2. In turn, the N_2 sorption isotherm corresponding to the dimorphous SiO_2 reference material is shown in Fig. 3; the sorption isotherm of the latter substrate also portrays a series of primary desorption scanning curves (Fig. 3a).

The volume sorbed by the SiO_2 hybrid substrate at a given p/p^0 (see Fig. 3a) results from the contributions of the amounts adsorbed on the SBA-16 and SBA-15 pore domain masses that compose the solid of reference (i.e. the experimental isotherm of the dimorphous material is the precise sum of the respective contributions of the individual SBA-15 and SBA-16 weight fractions):

$$V_{hybrid}(p/p^0) = m_{SBA-16}\, V_{SBA-16}(p/p^0) + m_{SBA-15}\, V_{SBA15}(p/p^0) \quad (1)$$

where V_{hybrid} is the volume adsorbed by the dimorphous substrate, and $m_{\text{SBA-15}}$ and $m_{\text{SBA-16}}$ are the masses of the SBA-15 and SBA-16 silica materials that are present in the combined SiO_2 adsorbent, respectively.

As a consequence of the above additive property, the SiO_2 mixture of reference is undoubtedly constituted by independent pore domains, i.e. grains of cylindrical and spherical entities, which are filled with condensate (AB isotherm) at their own circumstance, irrespectively of what is happening in all remaining pores. Nevertheless, the DB branch follows a different behavior.

While the cylindrical pore entities can evaporate their condensate suffering no interference from their neighboring pores, the spherical entities are dispossessed of condensate in a different fashion. Spherical cavities evaporate their condensate at lower pressures if compared to cylindrical voids and are altogether emptied of liquid due to a percolation phenomenon; this

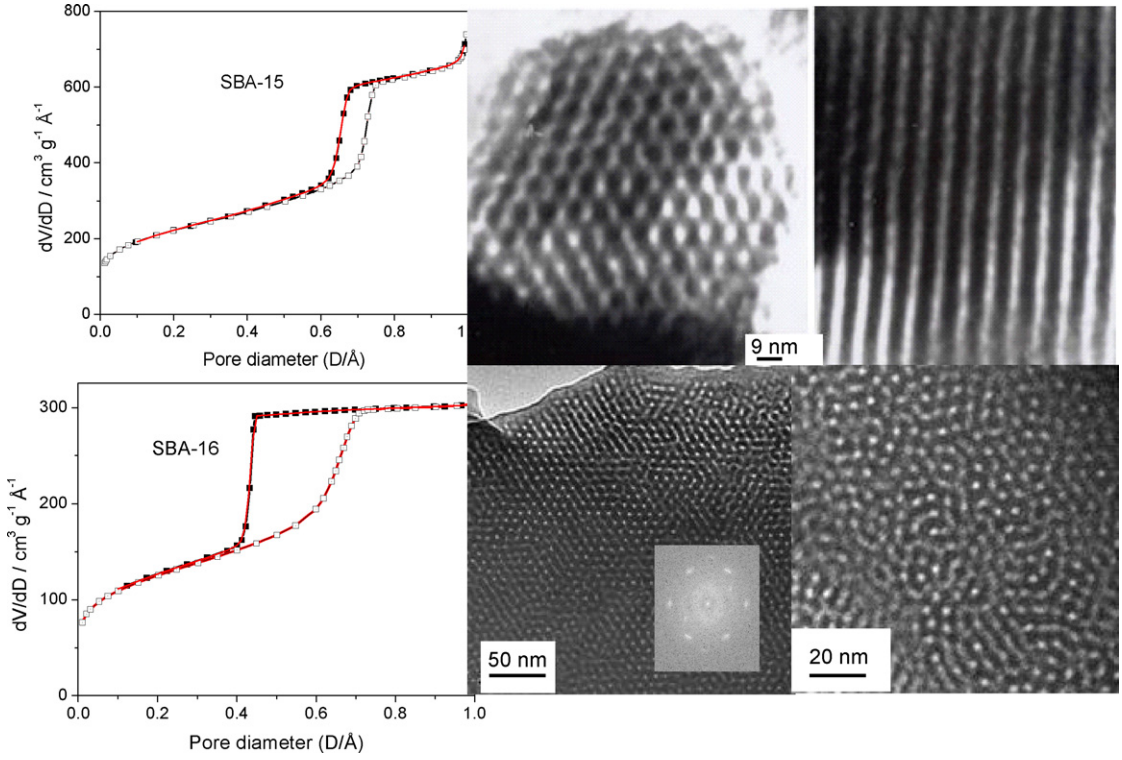

Fig. 2. N_2 sorption isotherms and HRTEM images of the SBA-15 and SBA-16 silica materials that compose the dimorphous SiO_2 reference material. The inset in one of the bottom images shows the electron diffraction pattern of the spherical SBA-16 pore array.

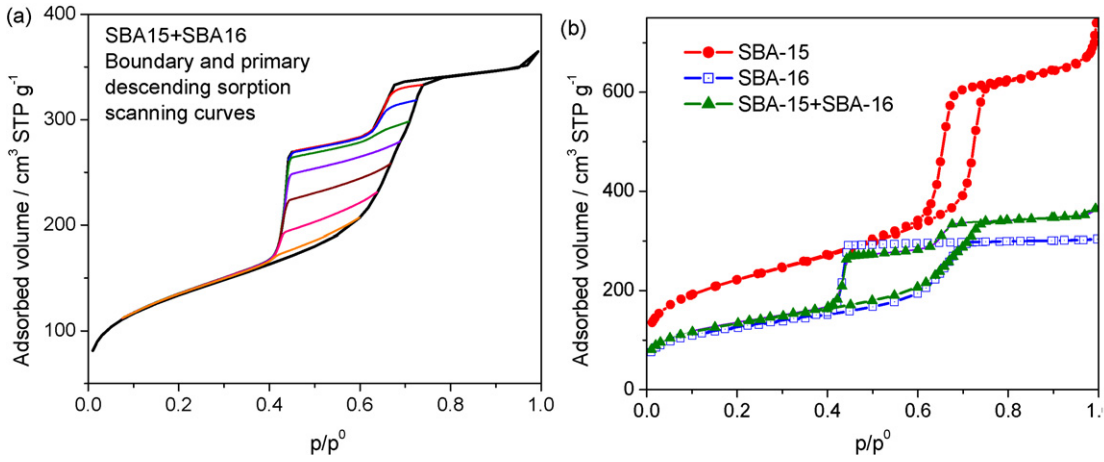

Fig. 3. (a) N_2 sorption isotherm at 76 K on the dimorphous SiO_2 reference sample. (b) SBA-15, SBA-16, and (SBA-15 + SBA-16) isotherm comparison. A set of primary desorption scanning curves is also depicted within the HL of the SiO_2 reference substrate.

process occurs mostly because of the fact that the spherical cavities are delimited by small openings (~2.3 nm in size). These necks act as stoppers to the exit of condensate until cavitation [8] (i.e. the spontaneous nucleation of vapor bubbles in the bulk of the condensate phase that is being retained in the spherical pores) surges at a given p/p^0 thus provoking a percolation phenomenon (i.e. the condensed phase suddenly evaporates from practically all pores of the substrate).

The pore size distributions (PSD) of the SBA-16 and SBA-15 substrates can be calculated from the sorption isotherms through the non-local density functional theory (NLDFT) method [9] and are shown in Fig. 4. The AB isotherms corresponding to the SBA-16 and the (SBA-15 + SBA-16) mixture allow the calculation of the sizes of the spherical chambers that are present in both samples. In turn, the DB isotherms associated to the SBA-15 and the (SBA-15 + SBA-16) hybrid mixture render the sizes of the cylindrical pores that are present in both substrates. Finally, it would be convenient to mention that the primary desorption curves, portrayed in the sorption isotherm of the dimorphous SBA-15 + SBA-15 reference material, are not asymptotically approaching the DB isotherm; this fact reflects the independent pore nature of the voids constituting the dimorphic sample [5].

4.2. Morphology of hybrid SiO_2 mesoporous solids as inferred from the appearances of the N_2 sorption isotherms and PSD curves and verification of these deductions from TEM observation

On the basis of the shapes depicted by the N_2 sorption isotherms of the SBA-15 and SBA-16 pore substrates (Fig. 2), the sorption curves related to the SiO_2 solids arising from the mixing of sol–gel dispersions of triblock P123 and F127 surfactants adopt, in general, hybrid uptake characteristics (Fig. 3). An overall panoramic view of the different shapes exhibited by these isotherms can be seen in Fig. 5. The sorption shapes plotted therein suggest the following predominant morphologies:

- SiO_2 adsorbents prepared by Route 1 consist of a collection of embryonic quasi-spherical pore domains (i.e. the HL shape corresponds to an H2 type).
- SiO_2 substrates prepared from Routes 2 and 3 are mostly made of dimorphic (spherical + cylindrical) pore domains; however, it seems that spherical pores are better defined in the sample proceeding from Route 2 than the voids formed in the sample obtained by Route 3.

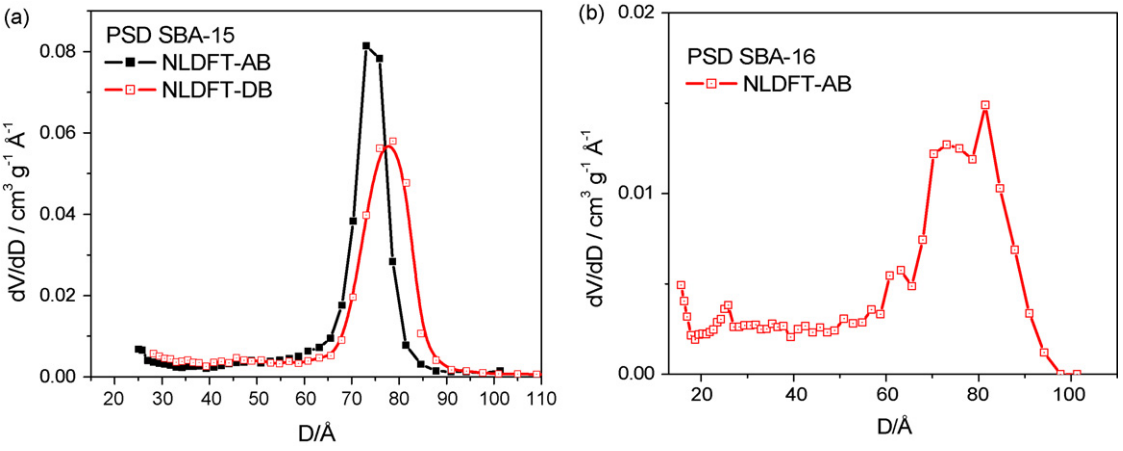

Fig. 4. (a) PSD of the SBA-15 pure silica sample calculated by the NLDFT approach [9] and applied to both ascending (AB) and descending (DB) boundary isotherms. (b) PSD of the SBA-16 pure silica sample calculated by the NLDFT treatment applied to the AB isotherm.

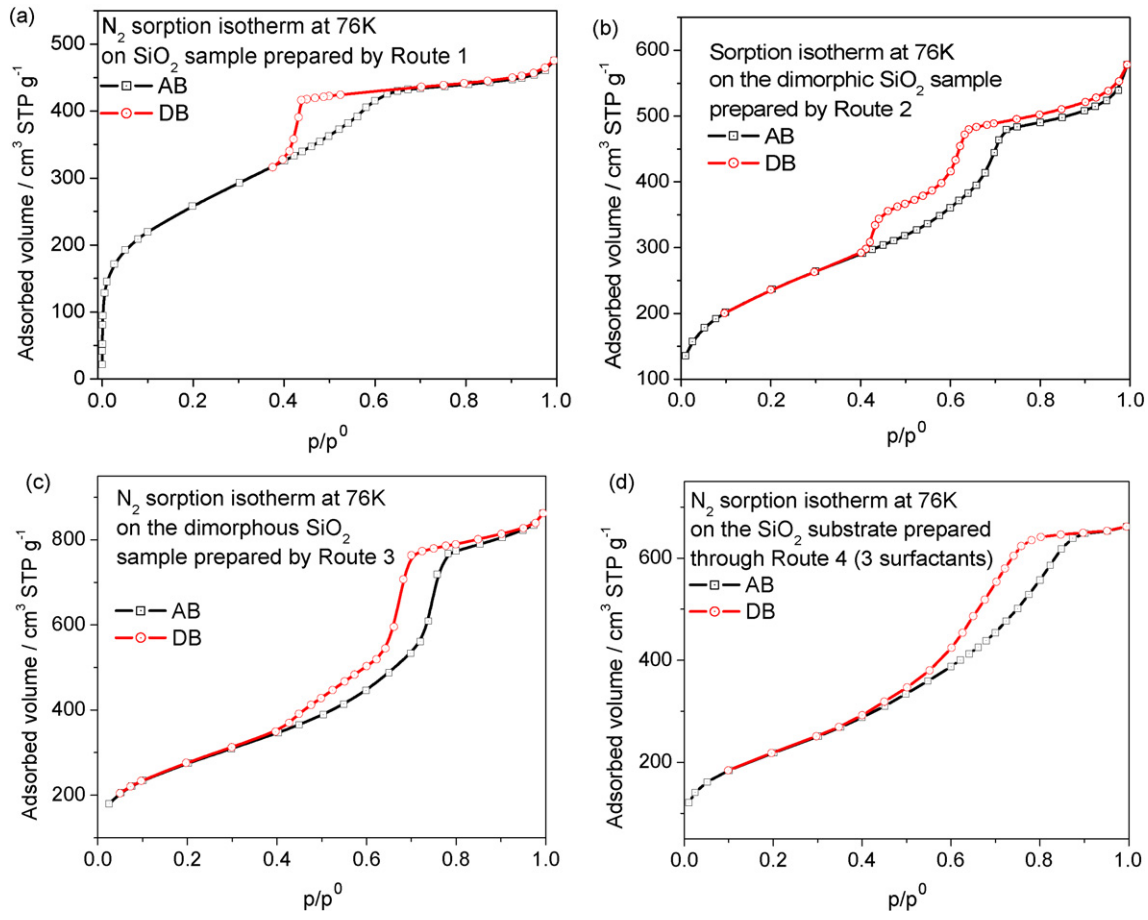

Fig. 5. Overall view of the N_2 sorption isotherms at 76 K on SiO_2 substrates arising from the mixing of sol–gel dispersions of P123 and F127 triblock surfactants. The isotherm shown in (d) corresponds to a SiO_2 solid prepared in the presence of P123, F127 and CTAB surfactants.

- SiO_2 materials synthesized by Route 4 are mostly tubular pore assemblages combined with some amount of embryonic spherical entities (this will be later confirmed from PSD results).

The above preliminary inferences, about the morphologies of the different hybrid SiO_2 substrates prepared through different routes, can then be confirmed (or not) from the corresponding TEM observation of the samples under analysis.

Fig. 6 shows that the SiO_2 sample prepared through Route 1 is constituted by solid grains containing spherical pores; the relatively long extent of the DB isotherm and the percolative appearance of the HL are just reflections of both the quasi-spherical characteristic of the pores and of the small pore necks that connect them to each other. In this sample there is no evidence at all about the presence of P123 cylindrical micelles (i.e. cylindrical pores are missing).

The substrate prepared through Route 2 can be seen (Fig. 7) to consist of separate granules of mesoporous cylindrical and spherical pore domains. The N_2 sorption isotherm of this sample (Fig. 5b) basically depicts the same main characteristics of the SBA-15 + SBA-16 reference material; the pores of the dimorphous material prepared by Route 2 are almost as well-defined as in the SiO_2 dimorphic material of reference, and the steps appearing along the AB and DB isotherms are similarly sharp and extensive as those appearing in the standard material. The PSD curve corresponding to cylindrical pores can be solved out from the DB isotherm (see Fig. 8); the PSD of the spherical voids cannot be inferred from the AB isotherm due to the simultaneous filling of spherical and cylindrical pores; however, a clear

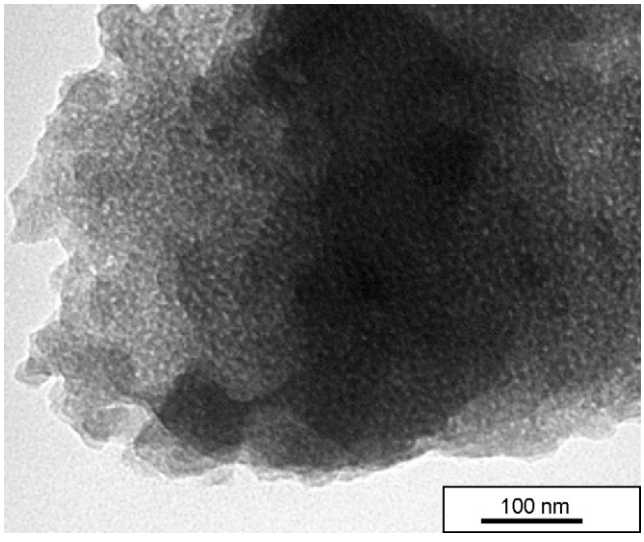

Fig. 6. TEM photograph of the SiO_2 sample prepared by Route 1. Spherical voids are seen to compose this substrate.

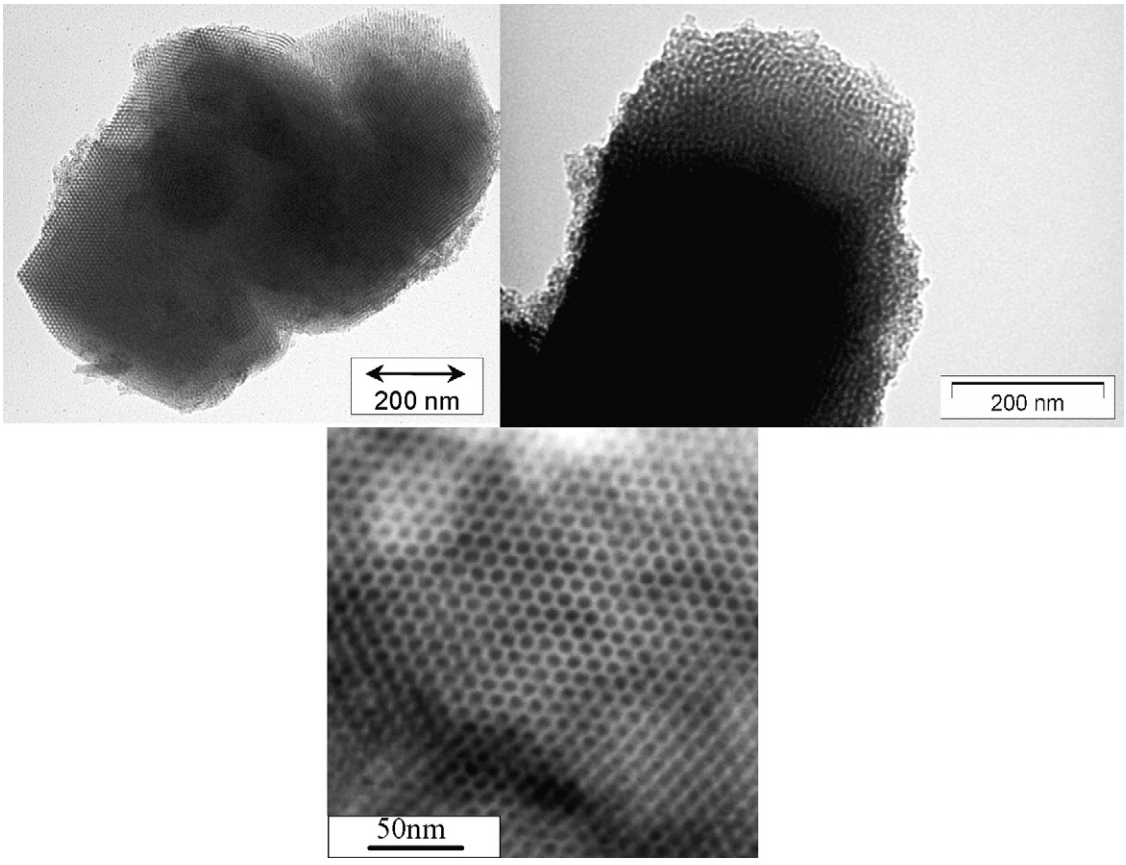

Fig. 7. TEM micrographs of cylindrical (top left) and spherical (top right) pore domains (grains) coexisting in the dimorphous SiO_2 mesoporous solid prepared through Route 2. The bottom image is a HRTEM photograph of the cylindrical pores.

hint that two pore shapes are involved in this sample is given by the shoulder of the PSD determined from the AB isotherm (Figs. 8a and b) through the NLDFT [9] treatment. This PSD shoulder cannot be discriminated into cylindrical and spherical pore contributions, since a single pore shape has to be assumed in order to perform the NLDFT calculation.

With respect to the hybrid mesoporous solid prepared through Route 3, one could have been expecting to find well-defined spherical and cylindrical pore domains by virtue of the relatively long aging times to which both micellar P123 and F127 dispersions had been subjected. Still, cylindrical pores of good aspect are evidently present but only embryonic (rather than extensive) domains of spherical pores can be seen in the TEM photographs of this sample (Fig. 9). The sorption isotherm thus depicts a sharp step along the DB isotherm, i.e. at $p/p^0 \approx 0.70$ where cylindrical pores are being emptied of condensate, as well as a sloping

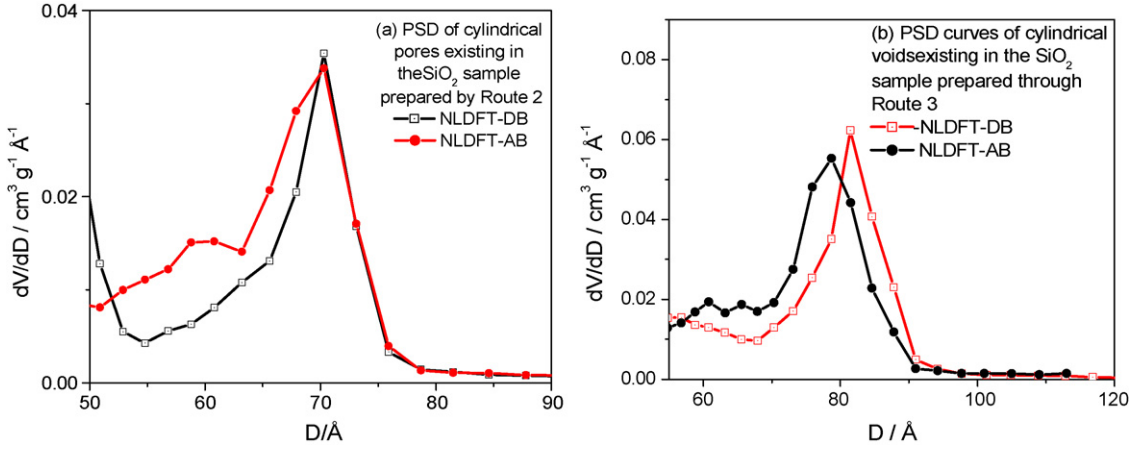

Fig. 8. (a) PSD curves of SiO_2 adsorbents prepared through Route 2 and (b) Route 3 and calculated according to the NLDFT approach. The divergence occurring in the 50–70 Å range between the PSD curves associated to both Routes is due to the concurrent filling of cylindrical and spherical voids during capillary condensation along the AB isotherm.

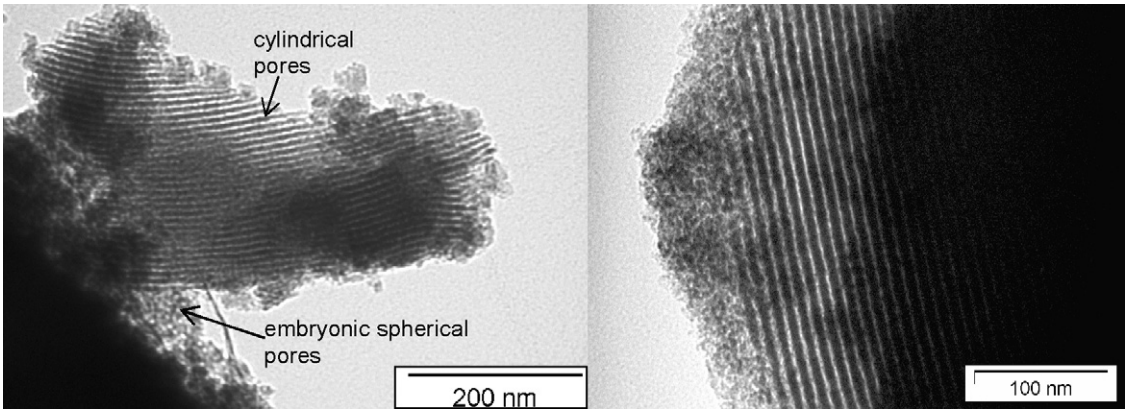

Fig. 9. TEM image showing the morphology of the SiO_2 material obtained through Route 3.

rather than a sudden collapse towards the lower p/p^0 part of the DB isotherm. This last characteristic suggests the existence of non-extensive domains of spherical voids, i.e. these pores are not too distant from the bulk vapor phase during a sorption experiment since they are not extensively interconnected to each other. Additionally, the TEM micrograph (Fig. 9) let us allow to see that some spherical entities appear at the grain boundaries between the cylindrical and spherical phases and that these spheroidal cavities seem to be in a significant deficit with respect to the number of cylindrical voids. Furthermore, there appear a variety of relatively small grain sizes containing spherical voids.

Finally, the morphology associated to the SiO_2 solid obtained through Route 4, shows cylindrical and quasi-spherical pore domains (Fig. 10). The P123 surfactant micelles have produced very definite cylindrical void zones, with the additional assistance of the CTAB molecules, which are also known to produce cylindrical micelles (of smaller diameters than those proceeding from the P123 surfactant). In contrast, the F127 micelles appear to have formed spherical pore grains of different extents (see TEM image in Fig. 10). This last assertion can be confirmed when looking at the DB branch of the HL since this curve approaches gradually but not suddenly to the AB isotherm, i.e. bubble cavitation is absent due to an apparent lack of pore throat interconnections among cavities. The PSD corresponding to cylindrical voids can be calculated from the DB isotherm (Fig. 10). The good coincidence between the PSD curves obtained from the AB and DB isotherms confirms that the dominant pore morphology in the SiO2 sample prepared through Route 4 should be the cylindrical one. Therefore, one can conjecture that the spherical entities observed in the TEM photograph are not too many or perhaps are incipiently formed. The relatively wide extent of the PSD also confirms that this sample is constituted by a wide range of tubular pores of different sizes (this fact could be caused by the synergetic effect between the P123 and CTAB surfactants) and also by the presumption that sorption by spherical cavities is almost negligible by reason of their insignificant number or their incipiently defined shape.

4.3. Pore structure parameters of dimorphic and monomorphic SiO_2 mesoporous adsorbents

The main pore structure parameters of the SiO_2 substrates synthesized in this work are summarized in Table 1. It is important to note the relatively high surface areas that most substrates display; the lowest one of these values corresponds to the SBA-16 adsorbent. The porosity also adopts prominent values and the presence of microporosity is almost negligible in most materials. The mean pore sizes and the PSD standard deviations are

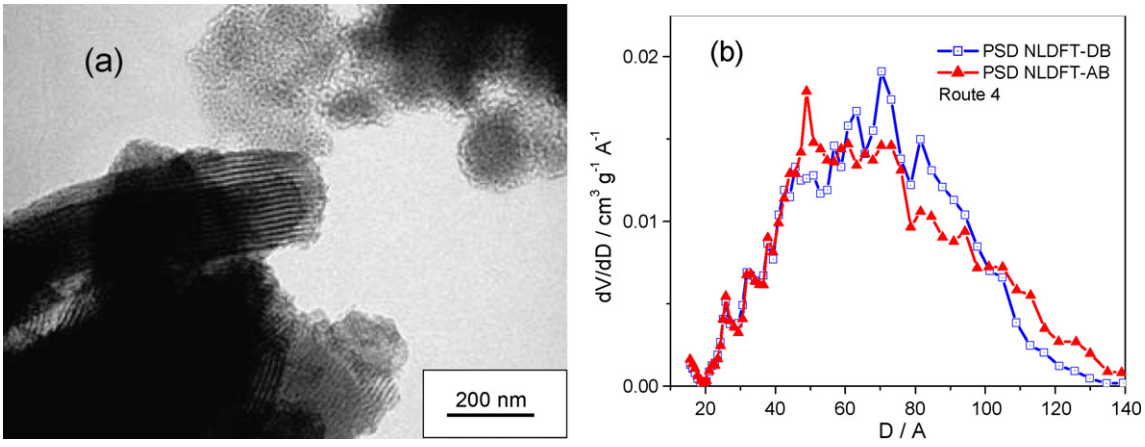

Fig. 10. (a) TEM image of the SiO_2 solid prepared from micellar dispersions of three surfactants (P123, F127, and CTAB, Route 4). Distinctive cylindrical and quasi-spherical pore domains are alternately found. (b) PSD curves calculated from the AB and DB N_2 isotherms on the SiO_2 solid prepared by Route 4.

Table 1
Pore structure parameters of dimorphic and monomorphic SiO_2 adsorbents

Adsorbent	BET surface area ($m^2\ g^{-1}$)	α_S-surface area ($m^2\ g^{-1}$)	Total pore volume ($mm^3\ g^{-1}$)	Micropore volume ($mm^3\ g^{-1}$)	Porosity (%)	Mean pore diameter $\pm\sigma$ nm
SBA-15	794	699	1009	41	69	74.2 ± 2.9 AB cyl, 77.4 ± 4.4 DB cyl
SBA-16	446	377	464	30	50.5	76.7 ± 10.1 sph
SBA-15 + SBA-16	479	417	537	27	54.2	73 AB, 77 DB cyl
SiO_2 Route 1	937	959	698	0	60.6	70.4 ± 10 sph
SiO_2 Route 2	895	839	860	20	66.3	70.7 AB cyl 70.4 DB cyl
SiO_2 Route 3	993	1006	1265	0	73.6	78.2 ± 5 AB cyl, 81.7 ± 3.9 DB cyl
SiO_2 Route 4	781	802	1004	0	68.8	65.7 ± 24.5 AB cyl, 68.7 ± 28.7 DB cyl

The α_S-surface areas are calculated from Gregg and Sing's α_S-plots [10]. σ is the standard deviation. The AB and DB acronyms stand for the mean pore diameters calculated from the AB and DB isotherms, respectively. The sph and cyl acronyms mean the pore shape, i.e. spherical or cylindrical.

also listed in Table 1; these parameters provide an idea about the size differences between spherical and cylindrical pores and of pore size ranges.

4.4. X-ray diffraction patterns

XRD patterns of some SiO_2 substrates are shown in Fig. 11. For the SBA-15 and SBA-16 substrates the d_{100} plane reflection occurs at 2θ values of 1.01° and 0.99°, respectively. Application of Bragg's law to these diffraction angles renders d_{100} distances of 87.2 and 89.1 Å, these values can be compared with the mode pore sizes of these samples, namely 78 and 76.7 Å. The difference between d_{100} distances and the mode pore sizes can be ascribed to the thickness of the pore walls [11]. Compared to the monomorphic SBA-15 and SBA-16 substrates, the XRD patterns of dimorphic substrates are not as sharp. Particularly, the d_{100}, d_{110}, and d_{200} plane reflections become shallower in the dimorphous materials than in the individual SBA-15 and SBA-16 pore systems. The low-angle d_{100} XRD signal corresponding to arrangements of spherical pores seems to be very sensitive to the presence of cylindrical pore domains, since even the reference SBA-15 + SBA-16 material shows no evidence of this peak, which usually appears in the range $0.9° \leq 2\theta \leq 1°$). The SiO_2 substrate arising from the Route 3 preparation procedure indicates that diffraction by some cylindrical pore domains takes place at about 1.15°. By applying Bragg's law to this last diffraction angle, the d_{100} distance becomes 79 Å a value that is not too different from the 79–81 Å mode pore sizes obtained from the PSD of this sample.

The SiO_2 sample prepared by Route 4 (and that is known to be made of a wide collection of tubular pores of diverse sizes) shows negligible XRD signals in the interval $1° \leq 2\theta \leq 1.5°$; this could be due to the wide extent of pore sizes as well as to the

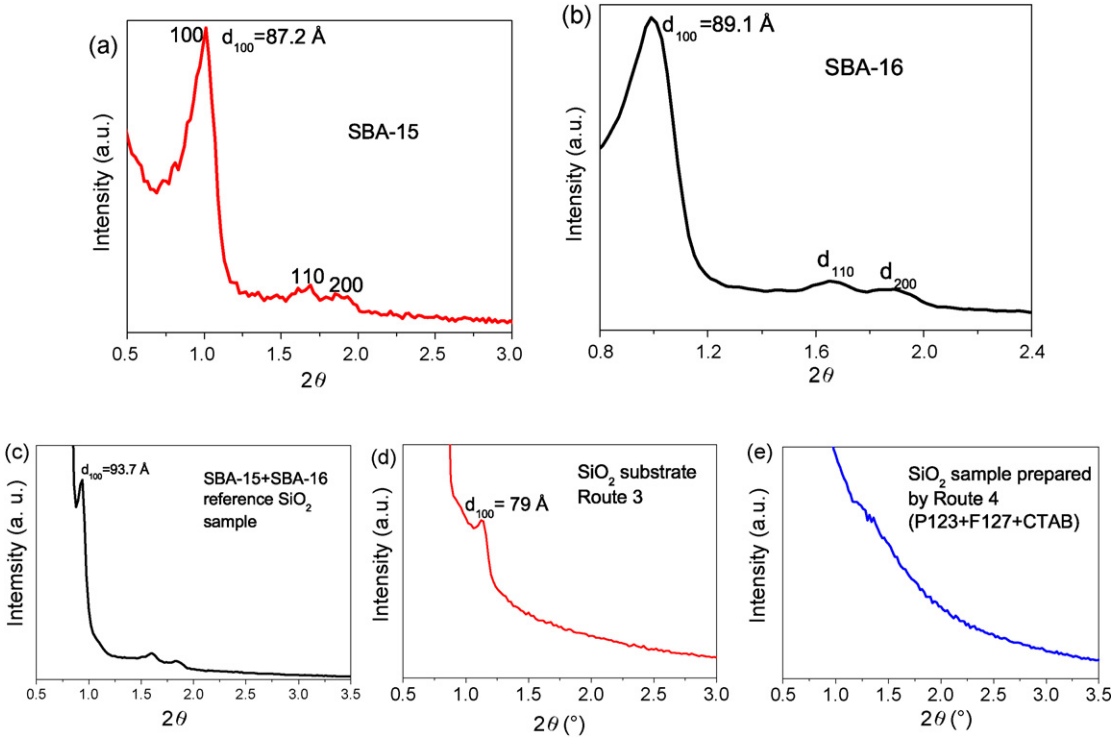

Fig. 11. XRD patterns of SiO_2 substrates. (a) SBA-15; (b) SBA-16, (c) SBA-15 + SBA-16 reference dimorphic sample, (d) dimorphic SiO_2 sample prepared by Route 3; (e) tubular SiO_2 substrate prepared by Route 4.

orientation disorder existing in the disposition of these pores throughout the sample.

5. Conclusions

The synthesis of mesoporous substrates from micellar dispersions of surfactants can accomplish the following pore arrangements:

- A monomorphic substrate made of spherical pores when F127 and P123 micellar surfactant dispersions are mixed together after each being aged for just 4 h. The cylindrical micelles, proper of the P123 substance, cannot be formed because of the interference of the F127 molecules.
- A dimorphic substrate consisting in a mixture of separate cylindrical and spherical pore domains is obtained when an aged P123 micellar dispersion is mixed with a fresh F127 dispersion. The inherent reason for attaining this dimorphous adsorbent lies on the contrasting gelling kinetics that the two surfactants exhibit; the F127 surfactant takes considerably longer to be organized in monodisperse micelles than the P123 compound does. The intrinsic value of this dimorphic sample is reflected in its two constituent shapes of pore entities that compose the solid.
- An interesting monomorphic substrate made of tubular pores of a wide size range is obtained after adding CTAB (Route 4) and F127 surfactants to a 4 h-aged dispersion of P123 surfactant aged for 4 h. Although this sample is not dimorphic, it still represents a particularly useful substrate since it is constituted by independent cylindrical pores within a wide range of sizes.
- Finally, the sample prepared by Route 3, which involved the mixing of two aged P123 and F127 gellifying masses rendered a partially dimorphic material. It seems that a longer aging period should be allowed to the F127 system to reach a more definite dimorphous adsorbent.
- The pore structure parameters of the SiO_2 materials arising from sol–gel mixtures of gellifying systems, such as surface area and porosity, display very convenient (large) values for the good development of a variety of physicochemical processes.

References

[1] Y. Kim, C. Kim, J. Yi, Mater. Res. Bull. 39 (2004) 2103–2112.
[2] A.B. Fuertes, D.M. Nevskaia, J. Mater. Chem. 13 (2003) 1843–1846.
[3] K.P. Gierszal, M. Jaroniec, Chem. Commun. (2004) 2576–2577.
[4] N. Nakamura, R. Takahashi, S. Sato, T. Sodesawa, S. Yoshida, Phys. Chem. Chem. Phys. 2 (2000) 4983–4990.
[5] D.H. Everett, in: E.A. Flood (Ed.), The Solid–Gas Interface, Dekker, New York, 1967, 1055–1113, Chapter 36.
[6] J.M. Esparza, M.L. Ojeda, A. Campero, G. Hernández, C. Felipe, M. Asomoza, S. Cordero, I. Kornhauser, F. Rojas, J. Mol. Catal. A: Chem. 239 (2005) 249–256.
[7] D. Grosso, A.R. Balkenende, P.A. Albouy, A. Ayral, H. Amenitsch, F. Babonneau, Chem. Mater. 13 (2001) 1848–1856.
[8] L. Sarkisov, P.A. Monson, Langmuir 17 (2001) 7600–7604.
[9] P.I. Ravikovitch, A.V. Neimark, Langmuir 18 (2002) 1550–1560.
[10] S.J. Gregg, K.S.W. Sing, Adsorption, Surface Area and Porosity, 2nd ed., Academic Press, London, 1982.
[11] M. Kruk, M. Jaroniec, Langmuir 15 (1999) 5279–5284.